Unraveling multifaceted roles of Grainyhead-like transcription factor-2 in breast cancer

Coban, B.

Chapter 4

GRHL2 regulation of growth/motility balance in luminal versus basal breast cancer

[1] Division of Drug Discovery and Safety, Leiden Academic Center for Drug Research, Leiden University, The Netherlands.

* Correspondence: Erik HJ Danen; e.danen@lacdr.leidenuniv.nl; Division of Drug Discovery and Safety, Leiden Academic Center for Drug Research, Leiden University, Einsteinweg 55, 2333CC Leiden, The Netherlands

Chapter 4

Abstract:

The transcription factor Grainyhead-like 2 (GRHL2) is a critical transcription factor for epithelial tissues that has been reported to promote cancer growth in some- and suppress aspects of cancer progression in other studies. We investigated its role in different breast cancer subtypes. In breast cancer patients, GRHL2 expression was increased in all subtypes and inversely correlated with recurrence-free and distant metastasis-free survival. In a large cell line panel, GRHL2 expression was expressed in luminal- and basal A cells but low or absent in basal B cells. Inter-section of ChIP-Seq analysis in 3 luminal and 3 basal A cell lines identified conserved GRHL2 binding sites for both subtypes. Pathway analysis of ChIP-seq data revealed cell-cell junction regulation and epithelial migration as well as epithelial proliferation as candidate GRHL2-regulated processes and further analysis of hub genes in these pathways showed similar regulatory networks in both subtypes. However, GRHL2 deletion in a luminal cell line caused cell cycle arrest while this was less prominent in a basal A cell line. Conversely, GRHL2 loss triggered enhanced migration in the basal A cells but failed to do so in the luminal cell line. ChIP-Seq and ChIP-qPCR demonstrated GRHL2 binding to CLDN4 and OVOL2 in both subtypes but not to other GRHL2 targets controlling cell-cell adhesion that were previously identified in other cell types, including CDH1 and ZEB1. Nevertheless, E-cadherin protein expression was decreased upon GRHL2 deletion especially in the luminal line and, in agreement with its selectively enhanced migration, only the basal A cell line showed concomitant induction of Vimentin and N-cadherin. To address how the balance between growth reduction and aspects of EMT upon loss of GRHL2 affected in vivo behavior, we used a mouse basal A orthotopic transplantation model in which the GRHL2 gene was silenced. This resulted in reduced primary tumor growth and a reduction in number and size of lung colonies, indicating that growth suppression was the predominant consequence of GRHL2 loss. Altogether, these findings point to largely common but also distinct roles for GRHL2 in luminal- and basal breast cancers with respect to growth and motility and indicate that, in agreement with its negative association with patient survival, growth suppression is the dominant response to GRHL2 loss.

1. Introduction

Breast cancer is the most prevalent malignancy in females globally. Mortality of patients with breast cancer has decreased, resulting from early diagnosis and development of therapies [1-3]. A considerable proportion of knowledge on breast cancer originates from experiments performed with breast cancer cells that cover the various subtypes of this heterogeneous disease [4]. Breast cancer is divided into luminal (luminal A and luminal B), epidermal growth factor receptor 2-enriched (HER2-enriched), basal (basal A and basal B), claudin-low, and normal-like subtypes based on gene expression profiling [5]. The most common subtype of breast cancer is luminal that originates from luminal cells in the duct [6]. It is characterized by enrichment of genes/proteins associated with the luminal epithelial phenotype (e.g., ESR1, GATA3 and FOXA1) [4,7]. Basal breast cancer is characterized by significant enrichment of basal epithelial cytokeratins, hormone receptor negativity and a high tumor grade and poor prognosis [8]. Basal breast cancer can be further divided into basal A and basal B subtypes [9]. The basal A subtype is enriched with basal markers such as cytokeratins (e.g., Cytokeratin 4), while basal-B exhibits a mesenchymal or a normal-like phenotype with overexpression of several genes related to tumor invasion and tumor stemness [4].

The Grainyhead (GRH) gene was originally discovered through a mutation that causes slack and fragile cuticles in Drosophila [10]. Loss of function of the GRH results in failure of neural tube closure during embryogenesis [11]. In mammals, members of the highly conserved Grainyhead like (GRHL) family directly or indirectly regulate transcription of the genes encoding epithelial cell-cell junction proteins in adherens junctions and tight junctions [12-14]. In humans, GRHL1, GRHL2 and GRHL3 are identified as GRH homologs that contain an N-terminal transcriptional activation domain, a central CP2 DNA-binding domain and a C-terminal dimerization domain [15,16]. GRHL2 has been found to serve as a pioneer factor, cooperating with FOXA1 and ERα to regulate gene expression [15,17,18]. >5000 GRHL2 binding sites have been reported in epithelial cells but there is limited overlap between different

tissues and regulation of several GRHL2 responsive genes has been found to be indirect [13,14,19-21].

GRHL2 has been implicated in cancer development and progression. GRHL2 has been shown to act as a tumor metastasis suppressor, by opposing epithelial-mesenchymal transition (EMT) through upregulation of epithelial markers or downregulation of mesenchymal markers [20,22,23]. In contrast, GRHL2 is located on chromosome 8q22 that is frequently amplified or overexpressed in many cancers and hence may rather have an oncogenic function [24-27]. Indeed, in prostate cancer [28], breast cancer [23], lung cancer [29] and ovarian cancer [30] downregulation of GRHL2 has been associated with inhibition of cell proliferation. Together, this suggests that GRHL2 function may vary depending on the cancer cell context.

In this study, we investigated the role of GRHL2 in different breast cancer subtypes. Our findings show that GRHL2 is absent in basal B breast cancer cells, it is expressed in luminal breast cancer cells where its depletion causes an arrested proliferation, and it is expressed in basal A where its depletion triggers a slow growth/high motility phenotype and in vivo, growth arrest is the dominant response to GRHL2 depletion, in line with its overexpression in breast cancer patients.

2. Results

2.1. GRHL2 is associated with poor prognosis but is downregulated in basal B subtype breast cancer

In order to evaluate the clinical relevance of GRHL2 in breast cancer, GRHL2 alternations were examined in a series of published cohorts. GRHL2 is located on chromosome 8q22.3, a genomic region that is frequently amplified or overexpressed in many cancers [25,28]. The expression of GRHL2 mRNA and protein was significantly higher in tumor versus normal tissue for all breast cancer subtypes analyzed (Fig. 1A, B). No statistically significant association of GRHL2 mRNA expression with overall survival was detected in luminal-like breast cancer (Fig. 2C). However, GRHL2 mRNA expression was negatively associated with overall survival in basal-like breast cancer patients (Fig. 2D). In agreement with an earlier report exploring a different panel of

cell lines [22], using RNA-seq data of 52 human breast cancer cell lines [35] we found that GRHL2 mRNA was low or absent in most breast cancer cell lines representing the basal B subtype and ex-pressed in all luminal and basal A cell lines (Fig. 2A, B). Notably, this analysis suggested that HCC1500 and SUM149PT may have been misclassified. Indeed, SUM149PT has been previously classified as basal A or basal B subtype [9,42] and reported to contain different subpopulations, according to expression level of EpCAM and CD49f surface markers [43]. Likewise, HCC1500 cells have been classified as luminal, due to a predominant population of cells that are positive for EpCAM and CD24 [3] or as basal B, owing to an enrichment for gene clusters associated with cancer stem cell- and invasive phenotypes [9]. In agreement with the RNA-seq analysis, GRHL2 protein and mRNA were not detectable in Hs578T basal B cells, whereas luminal (MCF7, T47D and BT474) and basal A cell lines (HCC1806, MDA-MB-468 and BT20) all expressed GRHL2, albeit at different levels (Fig. 2C, D). This was correlated with expression of E-cadherin, a cell adhesion receptor previously identified as a target of GRHL2 that is downregulated in cells undergoing EMT [23,44].
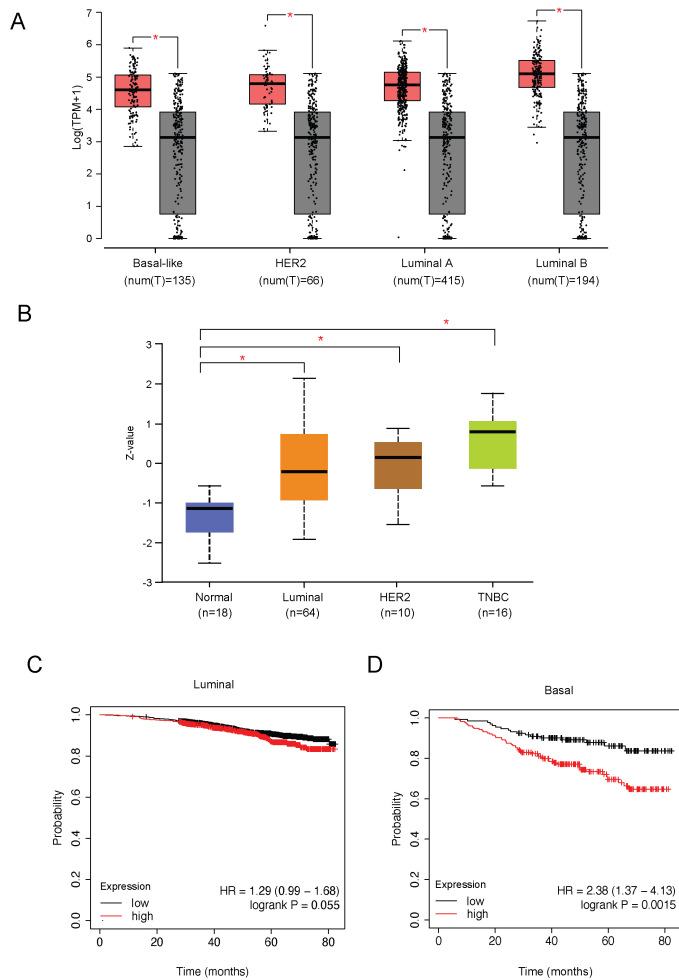
Fig. 1. GRHL2 expression in breast cancer. (A, B) The expression of GRHL2 mRNA **(A)** and protein **(B)** in different subtypes of breast cancer based on analyzing data from TCGA, GTEx and CPATC databases. TPM, transcripts per million. * Indicates p<0.01. Red and gray blocks in **(A)** represent tumor and normal samples, respectively. Dots show full distribution of all samples in the given group. **(C, D)** Association of GRHL2 expression with overall survival based on analyzing data from KM plotter database.
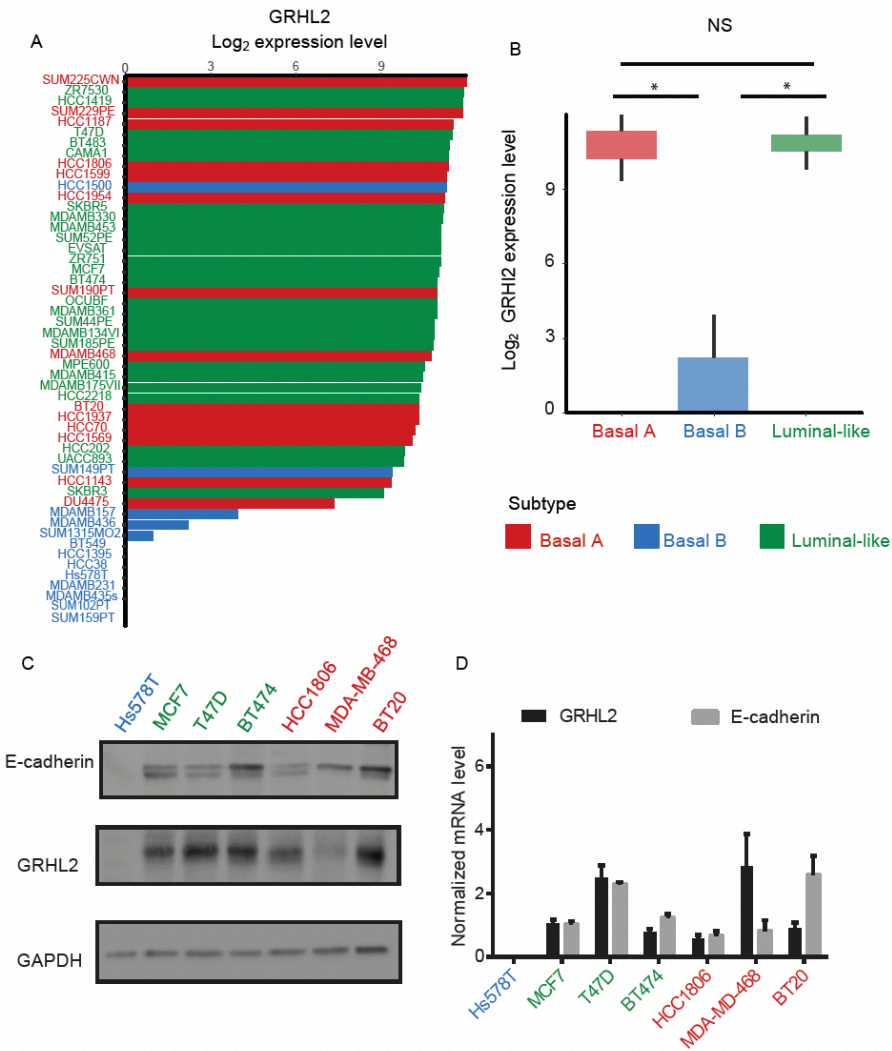
Fig. 2. GRHL2 expression in a panel of human breast cancer cell lines representing different subtypes. (**A** and **B**) GRHL2 expression in a panel of >50 human breast cancer cell lines covering luminal-, basal A-, and basal B subtypes extracted from RNA-seq data. * indicates p < 0.05; NS, not significant. (**C, D**) Western blot analysis (**C**) and qRT-PCR (**D**) showing loss of GRHL2 and its target gene CDH1 in basal B subtype breast cancer. Color codes refer to **B**.

2.2. Analysis of GRHL2-occupied genes in luminal and basal A breast cancer cells points to overlapping regulation of epithelial proliferation, cell-cell junctions, and cell migration

We performed ChIP-seq in three human luminal breast cancer cell lines and three human basal A breast cancer cell lines and identified 6527 shared GRHL2 binding sites in all luminal and 13351 shared GRHL2 binding sites in all basal A cell lines (Fig 3A). Of these, 4711 GRHL2 binding sites were shared between luminal and basal A cells. MEME-ChIP identified a core GRHL2 binding motif matching previously published motifs [14, 15, 17, 56] in each cell line (Fig. 3B). Annotation of ChIP-seq data in luminal and basal A cells revealed 3155 and 5353 Ensembl annotations for GRHL2 occupied genes, respectively. These genes were interrogated using the clusterProfiler package in R for GO term enrichment. Several GO terms associated with epithelial proliferation, cell-cell junctions, and cell migration were identified (Fig 3C). We combined GO terms associated with cell-cell junction/ adhesion or GO terms associated with epithelial cell migration from Fig. 3C and used Cytoscape (cytoHubba) to identify and select hub genes. The resulting hub gene networks were not identical but did show overlap between luminal and basal A cell (Fig. 3D). I.e., CDC42 and beta-catenin (CTNNB1) were shared between luminal and basal A in the cell-cell junction/ adhesion GO terms. CDC42, PTEN, EGF, and the VEGF receptor KDR (note that the ligand VEGFA was only found in basal A) were shared between luminal and basal A in the epithelial cell migration GO terms. Together, these analyses indicated that gene networks regulated by GRHL2 in luminal and basal A cells show large overlap and may regulate, amongst others, proliferation and cell migration of both subtypes.
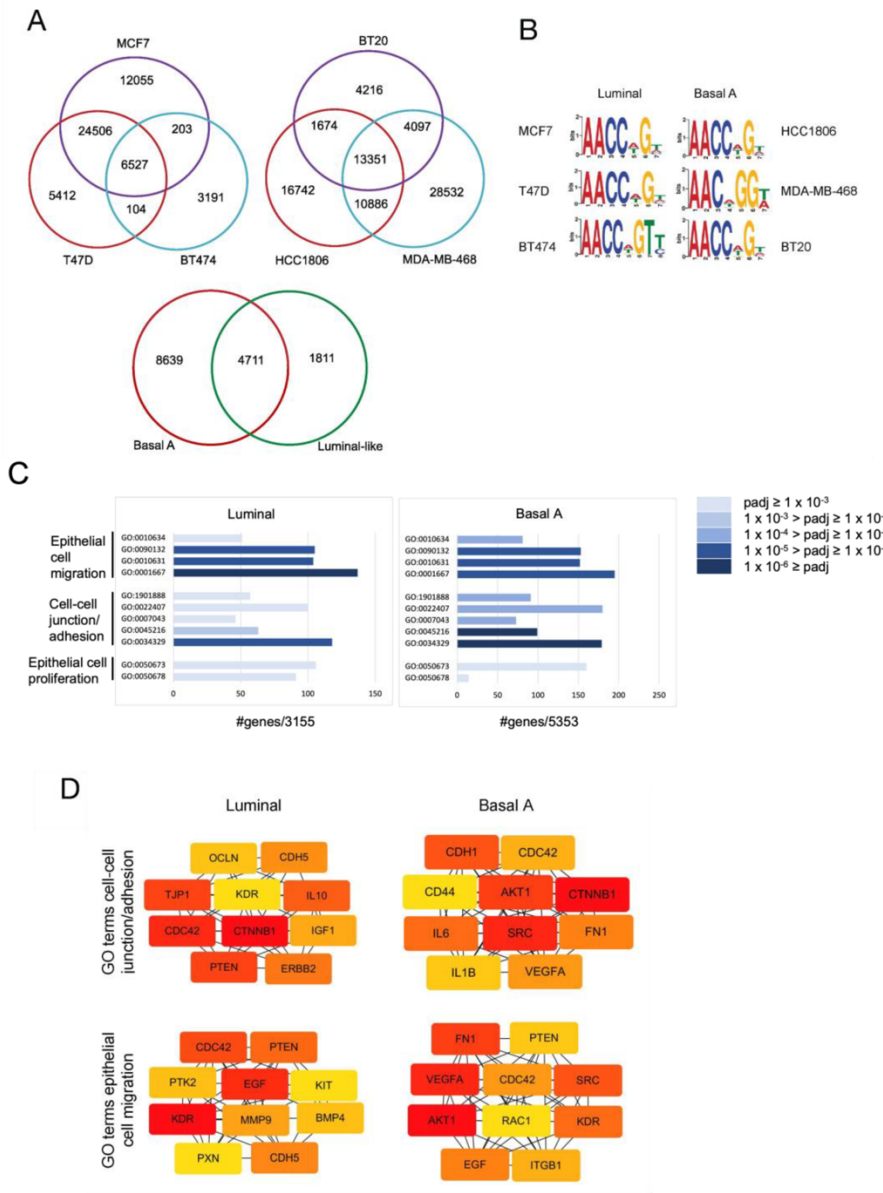
Fig 3. ChIP-seq analysis of GRHL2 target genes in luminal and basal A cells. (**A**) Venn diagrams showing overlap of GRHL2 binding sites among the indicated luminal and basal A cell lines (top panels) and overlap between shared GRHL2 binding sites in luminal and basal A cell lines (bottom panel). (**B**) GRHL2 DNA-binding

motifs identified in the indicated cell lines. (**C**) Enriched GO terms associated with the indicated functions for GRHL2-occupied genes shared between all luminal (left panel) or all basal A cell lines (right panel). Color coding according to padj values in the legend. X-axis shows the number of genes involved. (**D**) Hub genes calculated by Degree algorithm using Cytoscape (cytoHubba) software from the indicated GO terms for luminal and basal A cells. Color coding from red to yellow indicates the rank of the genes from top to low as assigned by cytoHubba.

2.3. Modulation of proliferation and migration in response to GRHL2 loss in luminal versus basal A breast cancer cells

GRHL2 has been shown to promote cell survival and proliferation and to suppress EMT in epithelial cells [2,22]. Our ChIP-seq analysis suggested that both aspects could be regulated in luminal as well as basal A breast cancer cells. We studied the response to GRHL2 loss in MCF7 luminal and HCC1806 basal A cells (Fig 4A). Cell cycle analysis showed that a higher percentage of MCF7 cells were in G0/1 compared to HCC1806 cells and loss of GRHL2 resulted in a G0/1 arrest in MCF7 and a less-pronounced shift to G0/1 in HCC1806 cells (Fig. 4B). In agreement with the more robust arrest in cell cycle progression observed in MCF7, loss of GRHL2 attenuated cell proliferation of MCF7 cells at 2- and 3-days post seeding whereas a smaller, albeit significant decrease in proliferation was observed at 3 days in HCC1806 (Fig. 4C). Conversely, when random migration was analyzed, migration speed of HCC1806 cells was enhanced upon GRHL2 depletion whereas migration of MCF7 was not significantly affected (Fig. 4D). Together, these results suggested that GRHL2 loss caused suppression of growth in both subtypes, especially in the luminal cells, that was accompanied by enhanced migration predominantly in the basal A subtype.
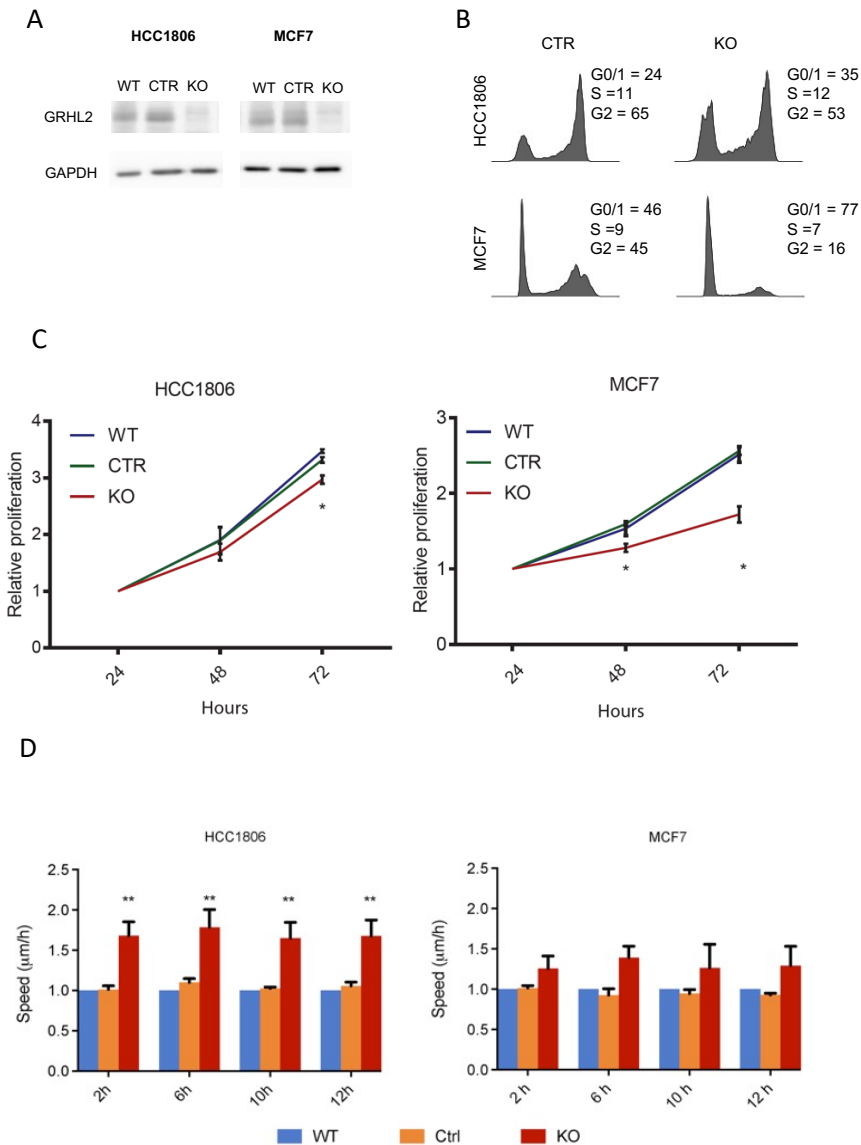
al- and basal A cells. (**A**) Western blot analysis showing loss of GRHL2 in KO cells. WT, wild type cells; CTR, sgCTR transduced cells; KO, sgGRHL2 transduced cells. (**B**) FACS profiles with associated quantification of cell cycle phase distribution in sgCTR (CTR) and sgGRHL2 transduced (KO) MCF7 and HCC1806 cells. Representative experiment from 2 and 3 biological replicates is shown for MCF7 and HCC1806, respectively. (**C**) Graphs showing results from SRB assay for wild type (WT) and sgCTR and sgGRHL2

127

transduced MCF7 and HCC1806 cells for the indicated time periods after 4 days doxycycline. Data are presented as mean ± SEM from 3 biological replicates. Data are statistically analyzed by t-test comparing CTR and KO to WT. * indicates p < 0.05. (**D**) Analysis of random migration assay showing the average path speed (y-axis) captured at the indicated timepoints during the assay (x-axis) for wild type (WT) and sgCTR and sgGRHL2 transduced MCF7 and HCC1806 cells 10-days post doxycycline. Data are presented as mean ± SEM from 3 biological replicates relative to WT. Data are statistically analyzed by two-way ANOVA. * indicates p < 0.05.

2.4. Signs of EMT in response to GRHL2 loss in luminal versus basal A breast cancer cells

We next asked whether the selective increase in migration speed triggered by GRHL2 loss in basal A but not luminal cells may be related to differential regulation of EMT. Analysis of ChIP tracks in luminal and basal A cell lines for previously reported GRHL2 target genes revealed high similarity amongst all six cell lines (Fig. 5A). No interactions of GRHL2 with ZEB1 or ZEB2 were detected in contrast to previous findings in mammary epithelial cells [45]. This was confirmed by ChIP-qPCR using a primer set reported to amplify ZEB1 promoter DNA sequences bound by GRHL2 in human mammary epi-thelial cells [22] (Fig. 5B). We also did not detect GRHL2 peaks associated with CDH2 (encoding N-cadherin, a mesenchymal marker). No promoter binding but multiple in-tronic GRHL2 peaks were detected in the CDH1 gene that were conserved in all cell lines and ChIP-qPCR confirmed one of these conserved intronic GRHL2 binding sites. Lastly, GRHL2 binding at the promoter regions of CLDN4 and OVOL2 was conserved in all cell lines and validated by ChIP-qPCR.
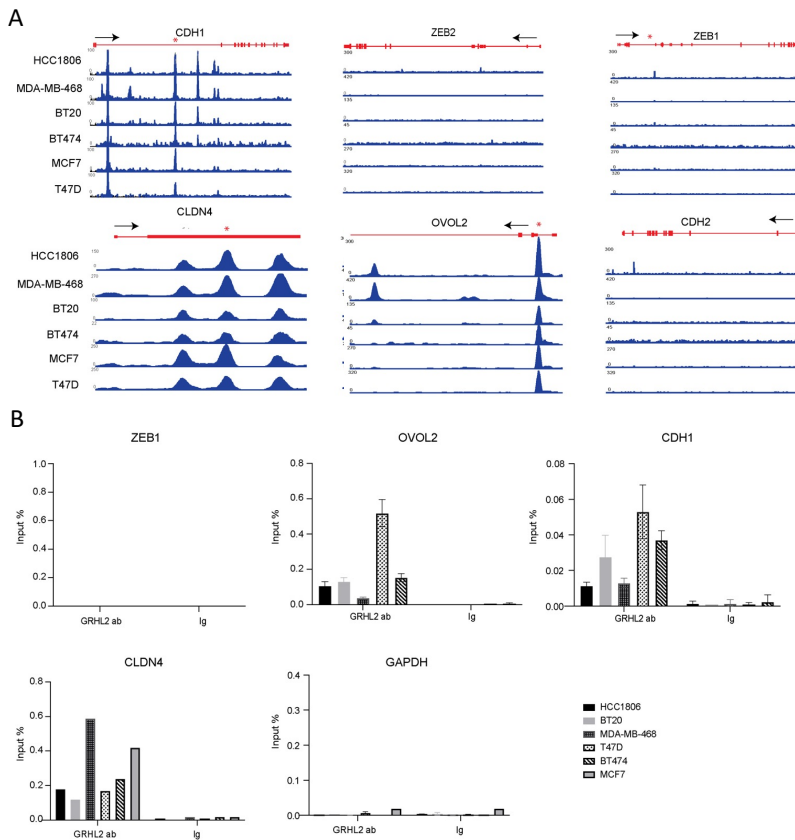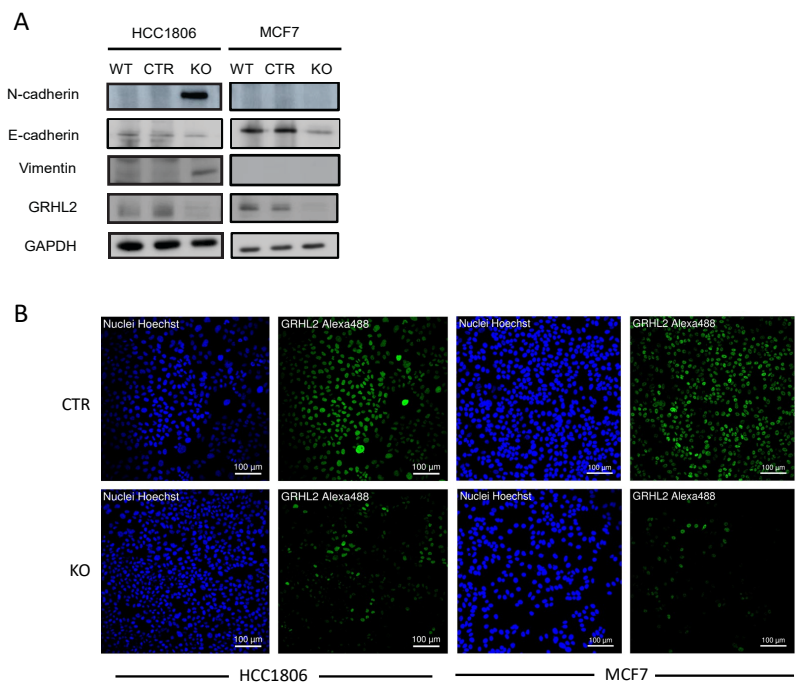
Fig. 5. Occupation of EMT related genes by GRHL2. (**A**) ChIP tracks for the indicated genes in luminal and basal A breast cancer cell lines. The track height is scaled from 0 to the indicated number. The locus with its exon/intron structure is presented in red. (**B**) ChIP-qPCR validation of presence and absence of GRHL2 binding sites identified by ChIP-seq. Location of the qPCR primer set in the locus is indicated by * in (**A**). Graphs represent the efficiency of indicated genomic DNA co-precipitation with anti-GRHL2 Ab or IgG control Ab. Signals for IgG control and GRHL2 antibody pulldown samples were normalized to input DNA and are presented as % input with SEM from 3 technical replicates with the exception of CLDN4 due to depletion of input material. Data were statistically analyzed by t-test and * indicates p < 0.05.

In addition to direct binding of regulators of EMT, GRHL2 may regulate EMT indirectly. In luminal (MCF7) and basal A cells (HCC1806) GRHL2 knockout, but not control sgRNA triggered a reduction in E-cadherin protein expression (Fig. 6A). However, the induction of mesenchymal markers, Vimentin and N-cadherin was only observed in HCC1806 cells. These Western blot results were confirmed using confocal immunofluorescence micros-copy. E-cadherin was expressed at cell–cell junctions and in the cytoplasm in HCC1806 and MCF7 cells and GRHL2 knockout led to reduced expression (Fig. 6B, C). A concomitant gain of Vimentin expression was only observed in HCC1806 cells. These results showed that direct binding of GRHL2 to EMT related genes is shared between luminal and basal A cells but GRHL2 depletion triggers several aspects associated with an EMT in HCC1806 whereas only reduction of E-cadherin is observed in MCF7, which may be in agreement with the enhanced migration observed in GRHL2-depleted HCC1806 but not MCF7 cells.
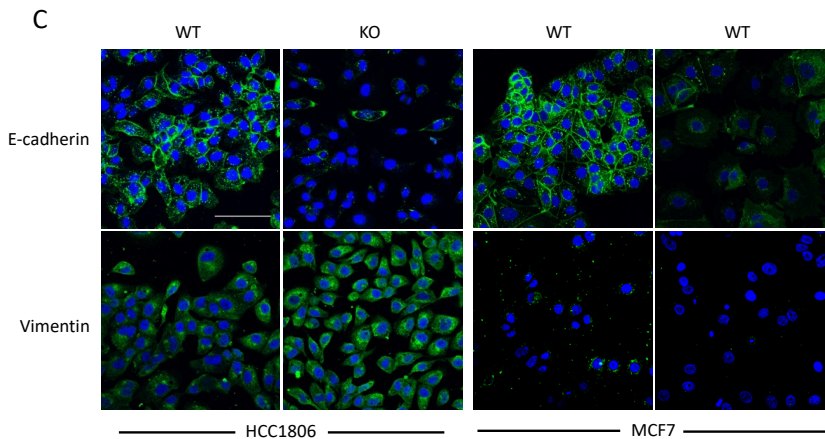
Fig. 6. Regulation of EMT related genes by GRHL2. (**A**) Western blot analysis of the indicated proteins in wild type (WT) and sgCTR (CTR) and sgGRHL2 transduced (KO) MCF7 and HCC1806 cells after 10 days doxycycline-induction. (**B**) Immuno-fluorescence analysis of HOECHST (nuclei, blue) and GRHL2 in MCF7 and HCC1806 cells expressing control sgRNA or GRHL2 sgRNA. **(C)** Immunofluorescence analysis of HOECHST (nuclei, blue), E-cadherin and Vimentin (Alexa-488, green), and F-ac-tin (Rhodamine-Phalloidin, red) in WT, CTR, and KO MCF7 and HCC1806 cells after 10 days doxycycline-induction. Scale bar, 100μm.

2.5. GRHL2 depletion leads to reduced tumor growth and lung metastasis of 4T1 basal A cells

A shift from an epithelial towards a mesenchymal phenotype contributes to metastasis [46]. We asked whether GRHL2 depletion in basal A cells would attenuate metastasis due to reduced growth potential or promote metasta-sis due to the EMT shift. For this purpose, we made use of the 4T1 mouse basal A orthotopic transplantation model. Expression of shRNAs targeting GRHL2 led to ~80% reduction in GRHL2 mRNA and caused a decrease in E cadherin expression (Fig. 7A, B). Orthotopic tumor growth of shGRHL2 cells was attenuated as compared to growth of shCTR tumors (Fig. 7C). Depletion of GRHL2 also reduced lung metastasis with fewer and very small lung colo-nies (Fig. 7D). These results indicated that the dominant outcome of GRHL2

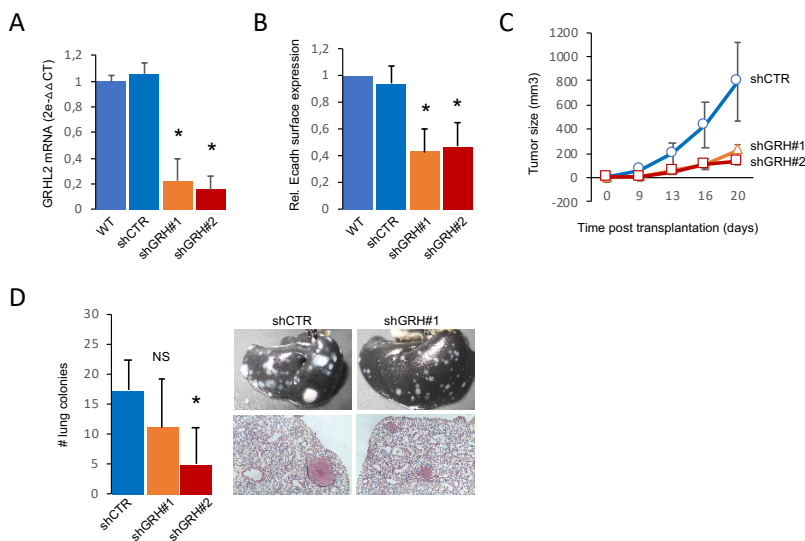loss in basal A breast cancer cells in the context of tumor growth and metastasis is growth suppression.

Fig. 7. Effect of GRHL2 depletion in 4T1 basal A orthotopic transplantation model. (**A**) RT qPCR analysis of efficiency of GRHL2 depletion in 4T1 cells transduced with a control or 2 GRHL2 shRNA constructs. Mean and SEM of 3 biological replicates is shown. * $p<0.05$. (**B**) FACS analysis of E cadherin surface expression in 4T1 variants described in A. Mean and SD of 3 experiments is determined and relative MFU (mean fluorescence units) compared to WT is shown. * $p<0.05$. (**C**) Graph showing mean and SD for analysis of primary tumor growth after orthotopic transplantation of control and GRHL2 shRNA transduced 4T1 cells. At least 12 mice per condition in two experiments were analyzed. (**D**) Graph showing mean and SD for number of detected lung colonies for the experiment as in (**C**). NS, not significant; * $p<0.05$. Right panel shows representative images of total lungs (top) and hematoxylin/eosin-stained lung sections derived from tumors of 4T1 cells transduced with a control or a GRHL2 shRNA construct.

3. Discussion

The results of this study indicate that the role of GRHL2 in luminal versus basal breast cancer cells is similar but not identical. Shared as well as distinct

gene sets are occupied by GRHL2 in these subtypes and the outcome of a reduction in GRHL2 ex-pression may be distinct with luminal cells experiencing a robust growth arrest and basal A cells maintaining a reduced growth potential that is accompanied by enhanced migration. Nevertheless, in agreement with its overexpression and negative correlation with survival in human basal-like breast cancer patients, loss of GRHL2 in basal A cells leads to reduced growth of orthotopic tumors and lung colonies, indicating that growth sup-pression is the dominant response to GRHL2 loss.

GRHL2 is located on chromosome 8q22 and amplified or overexpressed in several cancer types, including breast cancer [15,47]. In vivo and clinical studies support an oncogenic role of GRHL2 [15,27-30,48,49]. Our findings corroborate such a role for GRHL2 and demonstrate an association of GRHL2 expression with poor prognosis in breast cancer. Our study using a panel of >50 human breast cancer cell lines, confirms and extends an earlier report showing that GRHL2 is downregulated in basal B breast cancer [22]. This is remarkable given its apparent relation to poor prognosis, since triple negative/basal tumors are often aggressive and have a poorer prognosis compared to the ER-positive luminal subtypes [4]. Moreover, basal B cells are enriched in EMT markers that are also associated with aggressiveness [4].

GRHL2 may play a dual role in breast cancer [15,16,23] and a tumor- or metastasis-suppressive function has been related to its ability to suppress EMT, stemness, and invasion in cell line models and clinical samples [22,23,45]. The function of GRHL2 likely is context-dependent and the consequence of GRHL2 loss depends on the cancer type and the stage of cancer progression. Here, we have explored whether luminal- and basal A breast cancer cells that are GRHL2 positive and have an epithelial phenotype with E-cadherin-mediated cell-cell contacts, respond similarly to a loss of GRHL2. We find that GRHL2 downregulation negatively impacts growth and positively impacts aspects of EMT/migration in a luminal as well as a basal A cell line, but not to the same extent. Growth inhibition upon loss of GRHL2 is robust in MCF7 but less pronounced in HCC1806 cells. Notably, expression of PCNA and TERT, which has been reported to be epigenetically controlled by GRHL2 [26,50]

was attenuated in MCF7 but not HCC1806 cells following GRHL2 depletion, indicating that replicative potential is differentially affected (data not shown).

As expected, based on earlier reports in other cell types [21,51-53], E-cadherin is downregulated in response to GRHL2 knockout in luminal as well as basal A breast cancer cells. Our findings indicate that this response may be indirect. ChIP-seq and ChIP-qPCR detect intronic GRHL2-binding sites in the CDH1 gene but no promoter binding. By contrast, we find that genes encoding the epithelial tight junction protein, CLDN4 and the epithelial zinc finger protein, OVOL2 are subject to GRHL2 promoter binding. We do not detect GRHL2 binding sites in ZEB1 or ZEB2, across all the luminal and basal A breast cancer cell lines we have analyzed, which contrasts with previous findings in other cell types [45]. Hence, regulation of E-cadherin could involve OVOL2 but not ZEBs, in breast cancer cells. Notably, GRHL2 binding to noncoding gene regions, such as the intronic binding sites in CDH1, may participate in long-distance chromatin interactions [21]. Moreover, intronic regions harbor enhancer elements and GRHL2, in some cases together with the ER-alpha transcriptional complex, can act as a pioneer factor [15-18]. As the absence or presence of promoter or intronic binding sites is shared across the luminal and basal A cells, these interactions do not explain the different response to GRHL2 loss in both subtypes. On the other hand, we observe an induction of mesenchymal markers and enhanced cell migration only in GRHL2-depleted basal A HCC1806 cells and not in GRHL2-depleted MCF7 luminal cells. It has been previously shown that loss of E-cadherin is not sufficient for enhanced cell migration, invasion, and metastasis of breast cancer cells [54-56]. The induction of mesenchymal markers, such as N-cadherin and Vimentin that we find to occur only in the HCC1806 cells may contribute to cell migration. N-cadherin junctions on the cell surface may act as migration tracks [57] and N-cadherin supports the organization of an F-actin network that drives cell migration [58]. Again, the upregulation of N-cadherin in HCC1806 cells appears to be indirect as no GRHL2 bindings sites are detected in the CDH2 gene. Vimentin, a type III intermediate filament protein, is involved in cell adhesion, migration and signal transduction and emerges in pathologies processes involving epithelial cell migration [59] but overexpression of Vimentin

by itself does not enhance cell migration in MCF7 cells [60]. Altogether, our findings and other reports indicate that in order for GRHL2 loss to trigger a shift to a more motile behavior, loss of E-cadherin is not sufficient, but a more elaborate transition is required, including loss of epithelial markers and gain of mesenchymal markers.

Despite the induction of EMT and enhanced migratory capacity in basal A breast cancer cells the ultimate outcome of GRHL2 depletion in the orthotopic tumor growth and metastasis experiment reported here, supports an oncogenic role of GRHL2. This is in agreement with earlier studies [28,30,61] and with the fact that GRHL2 is located on chromosome 8q22 that is amplified or overexpressed in several cancer types, including breast cancer [15,47]. Our findings show that GRHL2 represents a candidate therapeutic target for luminal breast cancer. Even though growth of primary tumor and metastatic colonies derived from basal breast cancer cells is suppressed in response to GRHL2 depletion, the combination of reduced growth with aspects of EMT and enhanced motility does warrant caution with strategies aimed at decreasing expression of GRHL2 in basal breast cancer.

4. Materials and Methods

4.1. Expression analysis in breast cancer cohorts and cell line panel
 GRHL2 mRNA and protein expression in different subtypes were analyzed using GEPIA2 [31] and UALCAN [32,33], respectively. The KM plotter database was analyzed to evaluate the association of GRHL2 expression with survival of patients with different subclasses of breast cancer [34]. RNA-seq data for a panel of 52 breast cancer lines [35] was used to analyze GRHL2 expression across subtypes (basal A, basal B and luminal).

4.2. Cell lines
Human breast cancer cell lines (MCF7, T47D, BT474, HCC1806, BT20, MDA-MB-468, Hs578T) were obtained from the American Type Culture Collection. Cells were cultured in RPMI1640 medium with 10% fetal bovine serum, 25 U/mL penicillin and 25 µg/mL streptomycin in the incubator (37°C, 5% CO_2). For production of lentiviral particles, VSV, GAG, REV and Cas9 or sgRNA or shRNA plasmids were transfected into HEK293 cells using Polyethylenimine

(PEI). After 2 days, lentiviral particles were harvested and filtered. Conditional Cas9 cells were generated by infecting parental cells with lentiviral particles expressing Edit-R Tre3G promotor-driven Cas9 (Dharmacon) and selected by blasticidin. Limited dilution was used to generate Cas9 monoclonal cells. Subsequently, Cas9-monoclonal MCF7 or HCC1806 cells were transduced with U6-gRNA:hPGK-puro-2A-tBFP control non-targeting or GRHL2-specific single guide (sg)RNAs (Sigma), selected by puromycin, and gene deletion was triggered by exposure to doxycycline. Control sgRNA vector was non-targeting. Human GRHL2 sgRNA was CCTCGAGACAAGAGGCTGCTGTC. For shRNA transduction of 4T1 cells, cells were transduced using lentiviral shRNA vectors (LentiExpress; Sigma-Aldrich) according to the manufacturer's procedures and selected in medium containing puromycin (2 mg/ml). Control shRNA vector targeted enhanced green fluorescent protein. Mouse GRHL2 shRNAs were CGGAGAAATTTCGGAGTACTTCTC and CGTCCTT-GTTAA-GCGGATGTTCTC.

4.3. Western blot

Cells were lysed by radioimmunoprecipitation (RIPA) buffer (150 mM NaCl, 1% Triton X-100, 0.5% sodium deoxycholate and 0.1% Tris and 1% protease cocktail inhibitor (Sigma-Aldrich. P8340)). Then, cell lysates were sonicated and protein concentration was determined by bicinchoninic acid assay (BCA) assay. Cell lysates were mixed with protein loading buffer. Subsequently, proteins were separated by SDS-PAGE gel and transferred to methanol-activated polyvinylidene difluoride (PVDF) (Milipore, The Netherlands) membrane. Membranes were blocked with 5% bovine serum albumin (BSA, Sigma-Aldrich) for 1 hour at room temperature (RT). Membranes were stained with primary antibody overnight at 4°C and HRP-conjugated secondary antibodies for half hour at room temperature (RT). After staining with Prime ECL Detection Reagent (GE Healthcare Life science), chemoluminescence was detected by Amersham Imager 600 (GE Healthcare Life science, The Netherlands). The following antibodies were used: GRHL2 (At-las-Antibodies, hpa004820), GAPDH (SantaCruz, sc-32233), Vimentin (Abcam, ab8069), N-cadherin (BD, 610920), E-cadherin (Abcam, ab76055), Peroxidase AffiniPure Goat Anti-Rabbit IgG (Jackson ImmunoResearch, 111-035-003), Peroxidase

AffiniPure Goat Anti-Mouse IgG (Jackson ImmunoResearch, 115-035-003). Original blots are shown as supplemental data.

4.4. Realtime quantitative PCR (RT-qPCR)

Total RNA was isolated using RNeasy Plus Mini Kit (Qiagen). 500 ng RNA was reverse transcribed into cDNA using the RevertAid H Minus First Strand cDNA Synthesis Kit (Thermo Fisher Scientific). The cDNA was mixed with SYBR green master mix (Fisher Scientific) for qPCR. RT-qPCR data were collected and analyzed using 2−ΔΔCt method. RT-qPCR primers included GRHL2 forward ggcagtgtccttgttaaacgg / reverse atcgtcag-tctccttcctcacg; CDH1 forward: agagcttgtcattgagcctgg / reverse: ccacggatcttgtgtcagaaac; GAPDH forward: ccatggggaaggtgaaggtc/ reverse agttaaaagcagccctggtga.

4.5. ChIP-seq and ChIP-qPCR

Cells were grown in RPMI-1640 complete, serum-containing medium. Cross-linking was performed by 1% formaldehyde for 10 minutes at room temperature (RT). Then 1M glycine (141 µl of 1M glycine for 1 ml of medium) was used to quench for 5 minutes at RT. Cells were washed twice with ice-cold PBS containing 5 µl/ml phenylmethylsulfonyl fluoride (PMSF). Cells were harvested by centrifugation (2095 g for 5 minutes at 4°C) and lysed with NP40 buffer (150 mM NaCl, 50mM Tris-HCl, 5mM EDTA, 0.5% NP40, 1% Triton X-100) containing 0.1% SDS, 0.5% sodium deoxycholate and protease inhibitor cocktail (EDTA-free Protease Inhibitor Cocktail, Sigma). Chromatin was sonicated to an average size of 300 bp and GRHL2-bound chromatin fragments were immunoprecipitated with anti-GRHL2 antibody (Sigma; HPA004820). Precipitates were washed by NP buffer, low salt (0.1% SDS, 1% Triton X-100, 2mM EDTA, 20mM Tris-HCl (pH 8.1), 150mM NaCl), high salt (0.1% SDS, 1% Triton X-100, 2mM EDTA, 20mM Tris-HCl (pH 8.1), 500mM NaCl) and LiCl buffer (0.25M LiCl, 1%NP40, 1% deoxycholate, 1mM EDTA, 10mM Tris-HCl (pH 8.1)). Chromatin was de-crosslinked by 1% SDS at 65°C and DNA was purified by Phenol:Chloroform:Isoamyl Alcohol (PCI) and then diluted in TE buffer. Library preparation and paired-end (151bp) sequencing were performed by GenomeScan (Leiden, The Netherlands). MCF7, T47D, BT474, HCC1806, MDA-MB-468, and BT20 had 87393758, 84633440, 82080866, 89366122, 114657768, 62258090 paired-end reads, respectively. ChIP-seq

data are available at the UCSC Genome Browser [https://ge-nome.ucsc.edu/s/hwuRadboudumc/ZWang].

For ChIP-qPCR, the following primers were used: Control (an intergenic region upstream of the GAPDH locus): forward atgggtgccactggggatct / reverse tgccaaa-gcctaggggaaga; CLDN4: forward gtgacctcagcatgggctttga / reverse ctcctcctgaccagtttctctg; ZEB1 promoter: forward gccgccgagcctccaacttt / reverse tgctagggaccgggcggttt; OVOL2 exon: forward ccttaaatcgcgagtgagacc / reverse gtagcgagcttgttgacacc; CDH1 intron: for-ward gtatgaacggcaagcctctg / reverse caagggagccaggaagagaa. ChIP-qPCR data were an-alyzed using the 2−ΔΔCt method.

4.6. ChIP-seq analysis
Less than 5% of adapter sequences were present, and the mean per base sequence quality was >30, indicating high quality reads and no requirement for adapter-trimming. Paired-end reads were mapped to the human refer-ence genome (hg38) using BWA-MEM [36] with default parameters. Map-ping of total reads to the human genome for MCF7, T47D, BT474, HCC1806, MDA-MB-468, and BT20 was 42915, 36183, 10054,42554, 56906, 23486 re-spectively. Phred quality score (Q score) was used to measure base calling accuracy [37] and reads with low mapping quality (≤ Q30) were filtered out. MACS version 2.1.0 [38] was used for peak calling by default settings. The q value was adjusted to 0.1 for BT474 cell line to avoid loss of peaks. The an-notatePeaks and MergePeaks functions from HOMER [39] were used to an-notate and overlap peaks, respectively. ChIPseeker was used for the analysis of ChIP-seq peaks coverage plot and the density profile of GRHL2 binding sites [40]. Motif analysis was performed using ChIP-seq peaks with high scores by the MEME-ChIP program with default settings. ChIP-seq data was visualized by the UCSC genome browser.

The clusterProfiler package in R was used for GO enrichment analysis using the Kyoto Encyclopedia of Genes and Genomes (KEGG) database [41]. For this purpose, gene symbols of annotated ChIP-seq data were converted to Ensembl gene annotations. For the luminal and basal A subtypes 3155 and 5353 Ensembl annotations were analyzed, respectively. Protein-protein

interaction (PPI) networks were analyzed using STRING database (https://string-db.org/). The cytoHubba plugin in Cytoscape software (version 3.7.2) was used to identify hub genes and their networks. The "Degree" algorithm was used to select the top genes in Cytoscape.

4.7. Flow cytometry

Cell cycle analysis was performed with a Click-iT EdU Flow Cytometry Kit (Invitrogen). Cells were cultured with 50 µm 5-ethynyl-2-deoxyuridine (EdU) for 4 h and fixed and stained according to the manufacturers protocol for analysis on a BD FACS Canto II.

4.8. Sulforhodamine B (SRB) assay

Cell proliferation rate was measured by SRB assay. Cells were seeded into 96-well plates. At indicated time points, cells were fixed with 50% Trichloro-acetic acid (TCA, Sigma-Aldrich) for 1 hour at 4 °C and then plates were washed with demineralized water four times and air-dried at RT. Subsequently, 0.4% SRB (60 µl/well) was added and kept for at least 2 hours at RT. The plates were washed five times with 1% acetic acid and air-dried. 10 mM (150 µl/well) Tris was added and kept for half hour at RT with gentle shaking. The absorbance value was measured by a plate-reader Fluostar OPTIMA.

4.9. Migration assay

96 well-plates were coated with collagen (50 µl/well, 20 µg/ml) 1 hour 37°C and washed with PBS. Cells were seeded into the coated 96-well plates at the density of 8000 cells/well overnight and stained with Hoechst (Thermo Fisher 33242) diluted 1:7500 for 45 minutes. Images were taken every 5 minutes on a Nikon TE confocal microscope for 12 hours, at two positions per well. Tracks were analyzed using NIS Elements software and migration speed was calculated for 30 cells in each condition, tracked at 25 different timepoints.

4.10. Immunofluorescence

Cells were fixed with 2% formaldehyde for 15 minutes under slow rotation, permeabilized with 1% Triton in Phosphate buffered saline (PBS) for 10 minutes, and then stained with primary antibodies and secondary

antibodies. The following antibodies and stains were used: Vimentin (Abcam, ab8069); E-cadherin (Abcam, ab76055); GRHL2 (Atlas-Antibodies, hpa004820); Hoechst (33258, Abcam); Goat anti-Mouse IgG (H+L) Cross-Adsorbed Secondary Antibody-Alexa Fluor 488 (Thermo Fisher, A-11001); Rhodamine-Phalloidin (Thermo Fisher, R415).

4.11. Animal studies

Rag2−/−;gc−/− mice were housed in individually ventilated cages under sterile conditions. Housing and experiments were performed according to the Dutch guidelines for the care and use of laboratory animals. Sterilized food and water were provided ad libitum. Tumor cells (1×10^5) in 0.1 ml of phosphate-buffered saline were injected into the fat pad of 8- to 12-week-old female mice. Size of the primary tumors was measured using calipers. After 3 to 4 weeks, animals were anesthetized with pentobarbital. Lungs were excised and left lungs were fixed in 4% paraformaldehyde for hematoxylin and eosin staining. To quantify lung metastases, right lungs were injected with ink solution, destained in water, and fixed in Feketes [4.3% (v/v) acetic acid, 0.35% (v/v) formaldehyde in 70% ethanol].

4.12. Statistical analyses

Statistical analyses were performed by GraphPad Prism 8. Details are further de-scribed in the figure legends.

Data availability: Chip-seq data supporting the results of this article is available at the UCSC Genome Browser [https://genome.ucsc.edu/s/hwuRadboudumc/ZWang].

References

1. Harbeck, N. and Gnant, M. (2017) Breast cancer. Lancet 389, 1134-1150. 10.1016/S0140-6736(16)31891-8

2. Ma, L. et al. (2017) Grainyhead-like 2 in development and cancer. Tumour Biol 39, 1010428317698375. 10.1177/1010428317698375

3. Keller, P.J. et al. (2010) Mapping the cellular and molecular heterogeneity of normal and malignant breast tissues and cultured cell lines. Breast cancer research : BCR 12, R87. 10.1186/bcr2755

4. Dai, X. et al. (2017) Breast Cancer Cell Line Classification and Its Relevance with Breast Tumor Subtyping. J Cancer 8, 3131-3141. 10.7150/jca.18457

5. Dai, X. et al. (2015) Breast cancer intrinsic subtype classification, clinical use and future trends. American journal of cancer research 5, 2929-2943

6. Cancer Genome Atlas, N. (2012) Comprehensive molecular portraits of human breast tumours. Nature 490, 61-70. 10.1038/nature11412

7. Tran, B. and Bedard, P.L. (2011) Luminal-B breast cancer and novel therapeutic targets. Breast cancer research : BCR 13, 221. 10.1186/bcr2904

8. Prat, A. et al. (2015) Clinical implications of the intrinsic molecular subtypes of breast cancer. Breast 24 Suppl 2, S26-35. 10.1016/j.breast.2015.07.008

9. Neve, R.M. et al. (2006) A collection of breast cancer cell lines for the study of functionally distinct cancer subtypes. Cancer Cell 10, 515-527. 10.1016/j.ccr.2006.10.008

10. Ming, Q. et al. (2018) Structural basis of gene regulation by the Grainyhead/CP2 transcription factor family. Nucleic acids research 46, 2082-2095. 10.1093/nar/gkx1299

11. Nüsslein-Volhard C., W.E., Kluding H. (1984) Mutations affecting the pattern of the larval cuticle inDrosophila mel-anogaster : I. Zygotic loci on the second chromo-some. Wilehm Roux Arch Dev Biol. 193. 10.1007/BF00848156.

12. Werth, M. et al. (2010) The transcription factor grainyhead-like 2 regulates the molecular composition of the epitheli-al apical junctional complex. Development 137, 3835-3845. 10.1242/dev.055483

13. Aue, A. et al. (2015) A Grainyhead-Like 2/Ovo-Like 2 Pathway Regulates Renal Epithelial Barrier Function and Lu-men Expansion. Journal of the American Society of Nephrology : JASN 26, 2704-2715. 10.1681/ASN.2014080759

14. Walentin, K. et al. (2015) A Grhl2-dependent gene network controls trophoblast branching morphogenesis. Develop-ment 142, 1125-1136. 10.1242/dev.113829

15. Reese, R.M. et al. (2019) Grainyhead-like Protein 2: The Emerging Role in Hor-mone-Dependent Cancers and Epige-netics. Endocrinology 160, 1275-1288. 10.1210/en.2019-00213

16. Frisch, S.M. et al. (2017) Roles of Grainyhead-like transcription factors in cancer. Oncogene. 10.1038/onc.2017.178

17. Holding, A.N. et al. (2019) VULCAN integrates ChIP-seq with patient-derived co-expression networks to identify GRHL2 as a key co-regulator of ERa at enhancers in breast cancer. Genome biology 20, 91. 10.1186/s13059-019-1698-z

18. Cocce, K.J. et al. (2019) The Lineage Determining Factor GRHL2 Collaborates with FOXA1 to Establish a Targetable Pathway in Endocrine Therapy-Resistant Breast Can-cer. Cell Rep 29, 889-903 e810. 10.1016/j.celrep.2019.09.032

19. Gao, X. et al. (2013) Evidence for multiple roles for grainyhead-like 2 in the es-tablishment and maintenance of human mucociliary airway epithelium.[corrected]. Proc Natl Acad Sci U S A 110, 9356-9361. 10.1073/pnas.1307589110

20. Pifer, P.M. et al. (2016) Grainyhead-like 2 inhibits the coactivator p300, suppress-ing tubulogenesis and the epitheli-al-mesenchymal transition. Molecular biology of the cell 27, 2479-2492. 10.1091/mbc.E16-04-0249

21. Chung, V.Y. et al. (2016) GRHL2-miR-200-ZEB1 maintains the epithelial status of ovarian cancer through transcrip-tional regulation and histone modification. Scien-tific reports 6, 19943. 10.1038/srep19943

22. Cieply, B. et al. (2012) Suppression of the epithelial-mesenchymal transition by Grainyhead-like-2. Cancer research 72, 2440-2453. 10.1158/0008-5472.CAN-11-4038

23. Werner, S. et al. (2013) Dual roles of the transcription factor grainyhead-like 2 (GRHL2) in breast cancer. The Journal of biological chemistry 288, 22993-23008. 10.1074/jbc.M113.456293

24. Garnis, C. et al. (2004) Overexpression of LRP12, a gene contained within an 8q22 amplicon identified by high-resolution array CGH analysis of oral squamous cell carcinomas. Oncogene 23, 2582-2586. 10.1038/sj.onc.1207367

25. Dompe, N. et al. (2011) A whole-genome RNAi screen identifies an 8q22 gene cluster that inhibits death recep-tor-mediated apoptosis. Proc Natl Acad Sci U S A 108, E943-951. 10.1073/pnas.1100132108

26. Chen, W. et al. (2010) Grainyhead-like 2 enhances the human telomerase reverse transcriptase gene expression by in-hibiting DNA methylation at the 5'-CpG island in normal human keratinocytes. The Journal of biological chemistry 285, 40852-40863. 10.1074/jbc.M110.103812

27. Quan, Y. et al. (2014) Downregulation of GRHL2 inhibits the proliferation of col-orectal cancer cells by targeting ZEB1. Cancer Biol Ther 15, 878-887. 10.4161/cbt.28877

28. Paltoglou, S. et al. (2017) Novel Androgen Receptor Coregulator GRHL2 Exerts Both Oncogenic and Antimetastatic Functions in Prostate Cancer. Cancer research 77, 3417-3430. 10.1158/0008-5472.CAN-16-1616

29. Pan, X. et al. (2017) GRHL2 suppresses tumor metastasis via regulation of transcriptional activity of RhoG in non-small cell lung cancer. Am J Transl Res 9, 4217-4226

30. Faddaoui, A. et al. (2017) Suppression of the grainyhead transcription factor 2 gene (GRHL2) inhibits the prolifera-tion, migration, invasion and mediates cell cycle arrest of ovarian cancer cells. Cell Cycle 16, 693-706. 10.1080/15384101.2017.1295181

31. Tang Z, Li C, Kang B, Gao G, Li C, Zhang Z. GEPIA: a web server for cancer and normal gene expression profiling and interactive analyses. Nucleic Acids Res. Jul 3 2017;45(W1):W98-W102. doi:10.1093/nar/gkx247

32. Chandrashekar DS, Bashel B, Balasubramanya SAH, et al. UALCAN: A Portal for Facilitating Tumor Subgroup Gene Expression and Survival Analyses. Neoplasia. Aug 2017;19(8):649-658. doi:10.1016/j.neo.2017.05.00233. Chan-drashekar DS, Karthikeyan SK, Korla PK, et al. UALCAN: An update to the integrated cancer data analysis platform. Neo-plasia. Mar 2022;25:18-27. doi:10.1016/j.neo.2022.01.001

34. Gyorffy, B. et al. (2010) An online survival analysis tool to rapidly assess the effect of 22,277 genes on breast cancer prognosis using microarray data of 1,809 patients. Breast Cancer Res Treat 123, 725-731. 10.1007/s10549-009-0674-9

35. Koedoot, E. et al. (2021) Differential reprogramming of breast cancer subtypes in 3D cultures and implications for sensitivity to targeted therapy. Sci Rep 11, 7259. 10.1038/s41598-021-86664-7

36. Liu, C.M. et al. (2012) SOAP3: ultra-fast GPU-based parallel alignment tool for short reads. Bioinformatics 28, 878-879. 10.1093/bioinformatics/bts061

37. Ewing, B. et al. (1998) Base-calling of automated sequencer traces using phred. I. Accuracy assessment. Genome Res 8, 175-185

38. Zhang, Y. et al. (2008) Model-based analysis of ChIP-Seq (MACS). Genome biology 9, R137. 10.1186/gb-2008-9-9-r137

39. Heinz, S. et al. (2010) Simple combinations of lineage-determining transcription factors prime cis-regulatory ele-ments required for macrophage and B cell identities. Mol Cell 38, 576-589. 10.1016/j.molcel.2010.05.004

40. Yu, G. et al. (2015) ChIPseeker: an R/Bioconductor package for ChIP peak anno-tation, comparison and visualization. Bioinformatics 31, 2382-2383. 10.1093/bioin-formatics/btv145

41. Yu, G. et al. (2012) clusterProfiler: an R package for comparing biological themes among gene clusters. OMICS 16, 284-287. 10.1089/omi.2011.0118

42. Su, Y. et al. (2016) Development and characterization of two human triple-nega-tive breast cancer cell lines with highly tumorigenic and metastatic capabilities. Cancer Med 5, 558-573. 10.1002/cam4.616

43. Prat, A. et al. (2013) Characterization of cell lines derived from breast cancers and normal mammary tissues for the study of the intrinsic molecular subtypes. Breast Cancer Res Treat 142, 237-255. 10.1007/s10549-013-2743-3

44. Teo, K. et al. (2018) E-cadherin loss induces targetable autocrine activation of growth factor signalling in lobular breast cancer. Sci Rep 8, 15454. 10.1038/s41598-018-33525-5

45. Cieply, B. et al. (2013) Epithelial-mesenchymal transition and tumor suppression are controlled by a reciprocal feedback loop between ZEB1 and Grainyhead-like-2. Cancer research 73, 6299-6309. 10.1158/0008-5472.CAN-12-4082

46. Luond, F. et al. (2021) Distinct contributions of partial and full EMT to breast cancer malignancy. Developmental cell 56, 3203-3221 e3211. 10.1016/j.devcel.2021.11.006

47. Mlacki, M. et al. (2015) Recent discoveries concerning the involvement of tran-scription factors from the Grainyhead-like family in cancer. Experimental biology and medicine 240, 1396-1401. 10.1177/1535370215588924

48. Yang, X. et al. (2013) Bridging cancer biology with the clinic: relative expression of a GRHL2-mediated gene-set pair predicts breast cancer metastasis. PloS one 8, e56195. 10.1371/journal.pone.0056195

49. Butz, H. et al. (2014) Integrative bioinformatics analysis reveals new prognostic biomarkers of clear cell renal cell carcinoma. Clinical chemistry 60, 1314-1326. 10.1373/clinchem.2014.225854

50. Kang, X. et al. (2009) Regulation of the hTERT promoter activity by MSH2, the hnRNPs K and D, and GRHL2 in hu-man oral squamous cell carcinoma cells. Oncogene 28, 565-574. 10.1038/onc.2008.404

51. Chen, W. et al. (2018) Grainyhead-like 2 (GRHL2) knockout abolishes oral cancer development through reciprocal regulation of the MAP kinase and TGF-beta signaling pathways. Oncogenesis 7, 38. 10.1038/s41389-018-0047-5

52. Chen, W. et al. (2016) Grainyhead-like 2 regulates epithelial plasticity and stemness in oral cancer cells. Carcinogene-sis 37, 500-510. 10.1093/carcin/bgw027

53. Farris, J.C. et al. (2016) Grainyhead-like 2 Reverses the Metabolic Changes Induced by the Oncogenic Epitheli-al-Mesenchymal Transition: Effects on Anoikis. Mol Cancer Res 14, 528-538. 10.1158/1541-7786.MCR-16-0050

54. Sommers, C.L. et al. (1991) Cell adhesion molecule uvomorulin expression in human breast cancer cell lines: rela-tionship to morphology and invasive capacities. Cell growth & differentiation : the molecular biology journal of the Ameri-can Association for Cancer Research 2, 365-372

55. Truong, H.H. et al. (2014) beta1 integrin inhibition elicits a prometastatic switch through the TGFbeta-miR-200-ZEB network in E-cadherin-positive triple-negative breast cancer. Sci Signal 7, ra15. 10.1126/scisignal.2004751

56. Ilina, O. et al. (2020) Cell-cell adhesion and 3D matrix confinement determine jamming transitions in breast cancer invasion. Nat Cell Biol 22, 1103-1115. 10.1038/s41556-020-0552-6

57. Shih, W. and Yamada, S. (2012) N-cadherin-mediated cell-cell adhesion promotes cell migration in a three-dimensional matrix. J Cell Sci 125, 3661-3670. 10.1242/jcs.103861

58. Ponti, A. et al. (2004) Two distinct actin networks drive the protrusion of migrating cells. Science 305, 1782-1786. 10.1126/science.1100533

59. Ivaska, J. et al. (2007) Novel functions of vimentin in cell adhesion, migration, and signaling. Experimental cell re-search 313, 2050-2062. 10.1016/j.yexcr.2007.03.040

60. Sommers, C.L. et al. (1992) Loss of epithelial markers and acquisition of vimentin expression in adriamycin- and vinblastine-resistant human breast cancer cell lines. Cancer Res 52, 5190-5197

61. Hu, F. et al. (2019) Knockdown of GRHL2 inhibited proliferation and induced apoptosis of colorectal cancer by sup-pressing the PI3K/Akt pathway. Gene 700, 96-104. 10.1016/j.gene.2019.03.051
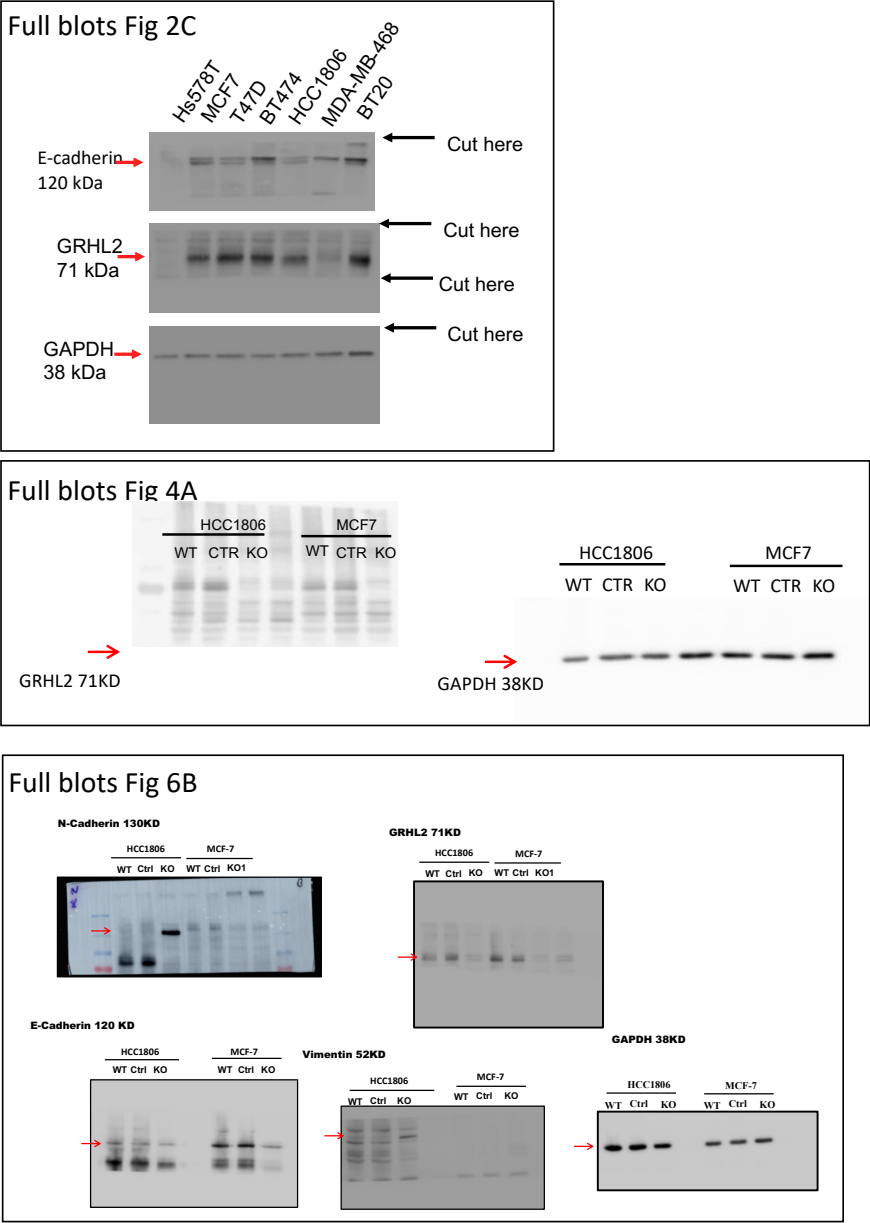
Supplementary Figures

Fig. S1. Full blots for Western blots shown in Fig **2C**, **4A**, and **6B**.